and blood levels are associated with more aggressive pituitary tumors (10, 11).

We identified altered FGFR4 expression in pituitary tumors (12) due to expression of an N-terminally deleted isoform, pituitary tumor-derived FGFR4 (13), generated by alternative transcription initiation from a cryptic intronic promoter (14, 15).

In a large cohort of pituitary neoplasms, strong FGFR4 protein expression was more frequently observed in larger adenomas (16). Subsequently, a common FGFR4 germline single nucleotide polymorphism that converts guanine to adenine, resulting in the substitution of arginine for glycine at codon 388 in the transmembrane domain, was identified (17). This FGFR4-R388 allele has been associated with poor outcomes in sarcoma (18); prostate (19), lung (20, 21), colon (17), and head and neck carcinomas (22); melanoma (23); and advanced breast cancer (24). Furthermore, we found that FGFR4-R388 was associated with more aggressive clinical behavior and diminished responsiveness to mammalian target of rapamycin inhibition therapy in patients with pancreatic neuroendocrine tumors (25).

We recently showed that the FGFR4-R388 allele modulates GH levels and is associated with larger pituitary tumor size in patients with acromegaly (26). Moreover, an independent clinical report noted that the FGFR4-G388 allele and FGFR4 overexpression were associated with a higher frequency of small microadenomas and recurrent Cushing disease (27). Cushing disease is a potentially lethal condition resulting from a pituitary corticotroph adenoma of the proopiomelanocortin (POMC)-derived ACTH cell lineage. Endowed with the capacity to stimulate adrenocortical hormone production, corticotroph tumors are clinically associated with elevated circulating cortisol levels (28). Most corticotroph tumors are small but very hormonally active, densely granulated basophilic adenomas; less frequently, they are larger, sparsely granulated chromophobic tumors with less prominent hormone hyperactivity, and up to 20% are regarded as silent corticotroph adenomas (SCA), clinically nonfunctioning pituitary adenomas with immunopositivity for ACTH (29). SCAs often exhibit a more aggressive clinical course (30–33).

In this report, we identify distinct signaling and hormone regulatory properties of the FGFR4-G388 and FGFR4-R388 isoforms of relevance to the different forms of Cushing disease.

## Materials and Methods

### Cell lines and cultures

Because there are no human-derived hormone-producing pituitary cell lines, we used mouse AtT20 corticotroph cells that were propagated in DMEM–10% fetal bovine serum (FBS) (Life Technologies), 1 mM sodium pyruvate, and 0.2 mg/mL G418 (37°C, 95% humidity, and 5% $CO_2$ atmosphere incubation).

### Plasmids and transfection

Plasmids encoding human prototypic FGFR4 (G388) or the polymorphic form FGFR4-R388 were generated and stably introduced into AtT20 cells as described previously (13). Construct fidelity was confirmed by DNA sequencing after introduction into pcDNA3.1. The signal transducer and activator of transcription (STAT) 3 expression vector was kindly provided by M. Minden (University of Toronto, Toronto, ON, Canada); the constitutively active tyrosine form of STAT3 (STAT3-CA) and constitutively active serine form of STAT3 (STAT3-S727D) were kindly provided by J. Chen (University of Illinois, Urbana, Illinois) (34). Cells were transfected using Lipofectamine 2000 (Life Technologies) according to the manufacturer's instructions. Stable clones were selected using neomycin (G418) at a concentration of 0.2 mg/mL. At least 3 clones of each isoform were used for further analyses.

### Cell treatments

Treatments with dexamethasone (2–25 nM; Sigma-Aldrich) were performed on cells grown on 100-mm plates ($3.5 \times 10^6$ cells/plate) after 24 hours of preincubation in serum-free defined medium (DMEM with 0.5% albumin bovine factor V). Treatments with dexamethasone were based on earlier dose and time course studies ranging from 10 minutes up to 24 hours.

### Cell proliferation assay

Cells ($5 \times 10^4$ cells/well) were seeded in 12-well plates, and growth rates were determined by direct counting 1, 4, and 5 days after seeding using the Vi-Cell XR 2.03 program of the Beckman Coulter system. Cells were also stained for Ki67 scoring as an additional measure of proliferation. Experiments were performed on 3 independent occasions, and each was performed in triplicate.

### Growth in soft agar

A total of 2500 cells were plated in 35-mm dishes as a single cell suspension in 0.3% agar in DMEM supplemented with 10% FBS over an underlayer of 0.5% agar prepared in DMEM as above. Colony formation was monitored daily with a light microscope, and colonies were photographed 3 weeks later. Each cell type (control, FGFR4-G388, or FGFR4-R388) was grown in 4 to 6 soft agar plates in each experiment.

### Western blotting and antibodies

Nuclear and cytoplasmic protein samples were prepared using NE-PER nuclear and cytoplasmic extraction reagents (Thermo Fisher Scientific). Cells were lysed in lysis buffer (0.5% sodium deoxycholate, 0.1% SDS, 1% Nonidet P-40, and 1× PBS) containing proteinase inhibitors (100 μg/mL phenylmethylsulfonylfluoride, 13.8 μg/mL aprotinin (Sigma-Aldrich), and 1 mM sodium orthovanadate (Sigma-Aldrich). Total cell lysates were incubated on ice for 30 minutes, followed by microcentrifugation at 10 000 × *g* for 10 minutes at 4°C. Protein concentrations of the supernatants were determined by the Bio-Rad method. Equal amounts of protein (40 μg) were mixed with 5× SDS sample buffer, boiled for 5 minutes, separated on 10 or 15% SDS-PAGE columns, and transferred onto polyvinylidene difluoride membranes. Immunoblotting was performed using the following antibodies: a monoclonal antibody to the V5-tag

(Life Technologies); anti-ACTH (1:10 000; Abcam); anti-B23 (1:5000; Sigma-Aldrich); anti-glucocorticoid receptor (GR) (BuGR2, 1:5000; Abcam); and GAPDH (1:1000), anti-pGR (Ser211, 1:1000), anti-pSrc (Y416, 1:1000), anti-pS-STAT3 (S727, 1:1000), anti-pY-STAT3 (Y705, 1:1000), anti-Src (1:1000), anti-STAT3 (1:2500) (Cell Signaling Technology). Loading was monitored by detection of actin (1:5000; Sigma-Aldrich). Nonspecific binding was blocked with 5% nonfat milk in 1× TBST (Tris-buffered saline with 0.1% Tween 20). After being washed 3 times for 10 minutes each in 1× TBST, blots were exposed to the secondary antibody (anti-mouse or anti-rabbit IgG-horseradish peroxidase; Santa Cruz Biotechnology) at a dilution of 1:2000 and were visualized using the ECL chemiluminescence detection system (Amersham). Protein band intensities were quantified by a scanning densitometer.

### Preparation of cell pellets for immunohistochemistry

Cell were washed 3 times in cold PBS, gently scraped, and centrifuged into pellets. The pellets were fixed in 10% formalin for 2 hours, coated in 2% Bacto Agar until solidified, fixed in 10% formalin, and embedded in paraffin. Sections of 4-$\mu$m thickness were dewaxed in 5 changes of xylene and rehydrated through graded alcohols into water. Sections were microwave heated in Tris-EDTA buffer at pH 9.0 inside a pressure cooker. Endogenous peroxidase and biotin activities were blocked using, respectively, 3% hydrogen peroxide and an avidin/biotin blocking kit (Vector Laboratories). Sections were treated for 10 minutes with protein blocker (ID LABS) and then were incubated overnight with anti-ACTH mouse monoclonal antibody at 1:800 and anti-Ki67 antibody at 1:100.

### Immunofluorescence detection of phospho-GR

Cells were grown in 2-chamber slides and preincubated in serum-free defined medium for 16 hours. Cells were treated with 10 nM dexamethasone for 1 hour, washed twice with PBS, fixed with 4% formaldehyde–PBS for 10 minutes, and washed 3 times with PBS. Cells were permeabilized for 10 minutes in PBS with 0.2% Triton X-100 and blocked for 30 minutes with PBS containing 5% FBS. Cells were first incubated with rabbit anti-phospho-GR (1:100) for 30 minutes at room temperature, washed 3 times with PBS, subsequently incubated with anti-rabbit IgG Alexa Fluor 488 for 30 minutes at room temperature, washed 3 times with PBS, incubated with 4′,6-diamidino-2-phenylindole for 15 minutes, and washed 3 times with PBS. Coverslips were mounted in Fluoromount-G (Electron Microscopy Sciences) on glass slides. Cells were examined with a two-photon microscope (LSM 510 META NLO; Zeiss), equipped with a ×63 water-immersion objective lens and filters optimized for double-label experiments. Images were analyzed using the LSM IMAGE browser.

### Fgfr4-R385 knock-in mice and treatment

Fgfr4-R385 knock-in mice were generated using standard approaches as described previously (35). Mice were maintained on a pure C57BL/6 background. Genotyping was performed by PCR of genomic tail DNA (35). Dexamethasone (Sigma-Aldrich) was reconstituted in saline and injected ip at a dose of 5 $\mu$g/g body weight at 6:00 PM and again at 8:00 AM the next morning, and then tail blood was collected 1 hour later for determination of serum corticosterone levels using a commercially available assay (ALPCO Diagnostics).

### Human samples

Human pituitary tumors were retrieved from the files of the University Health Network and Toranomon Hospital with research ethics board approval from both institutions. All tumors had been fully characterized according to currently accepted criteria (29). Pituitary tumor size was based on the maximal diameter noted on magnetic resonance imaging. Microadenomas were defined as tumors of <10 mm in maximal diameter and macroadenomas as tumors of >10 mm. FGFR4 genotyping was performed on white blood cells obtained from the peripheral blood of the same patients as described previously (17).

### Ethics statement

The care of animals was approved by the institutional animal care facilities. Use of human pituitary tissue was approved by the research ethics boards of the University Health Network and Toranomon Hospital.

### Statistical analysis

Data are presented as means ± SD. Statistical analyses were performed using unpaired, two-sided $t$ tests or ANOVA followed by a post hoc test. $P \leq .05$ was considered statistically significant. For analysis of human pituitary tumors, Fisher exact test was applied.

## Results

### FGFR4-G388R modulates POMC production and cell proliferation

As described previously, FGFR4 is expressed in anterior pituitary cells (26) including corticotroph cells (Supplemental Figure 1A). To determine whether the FGFR4 polymorphic isoforms possess distinct functional properties in ACTH-producing pituitary cells, we compared the effects of FGFR4-G388 and FGFR4-R388 on pituitary hormone production in mouse AtT20 corticotroph tumor cells. FGFR4-G388 enhances production of POMC and its cleaved product ACTH (Figure 1, A and B). In contrast to the hormonal changes, AtT20 cells expressing FGFR4-R388 showed higher proliferative activity evidenced by direct cell counting (Figure 1C), Ki-67 labeling (Figure 1D), and colony formation in soft agar (Figure 1E).

### FGFR4 polymorphic variants support distinct STAT3 modifications

To examine the mechanisms underlying the observed cellular responses, we compared signaling differences in AtT20 cells expressing the 2 FGFR4 isoforms. Src phosphorylation at Y416 was appreciably higher in cells expressing FGFR4-R388 than in those expressing FGFR4-G388, whereas phosphorylation at Y527 was unchanged (Figure 2, A and B). Importantly, FGFR4-R388 cells show higher STAT3 serine phosphorylation at S727 (Figure 2, A and C). In contrast, FGFR4-G388 cells displayed higher

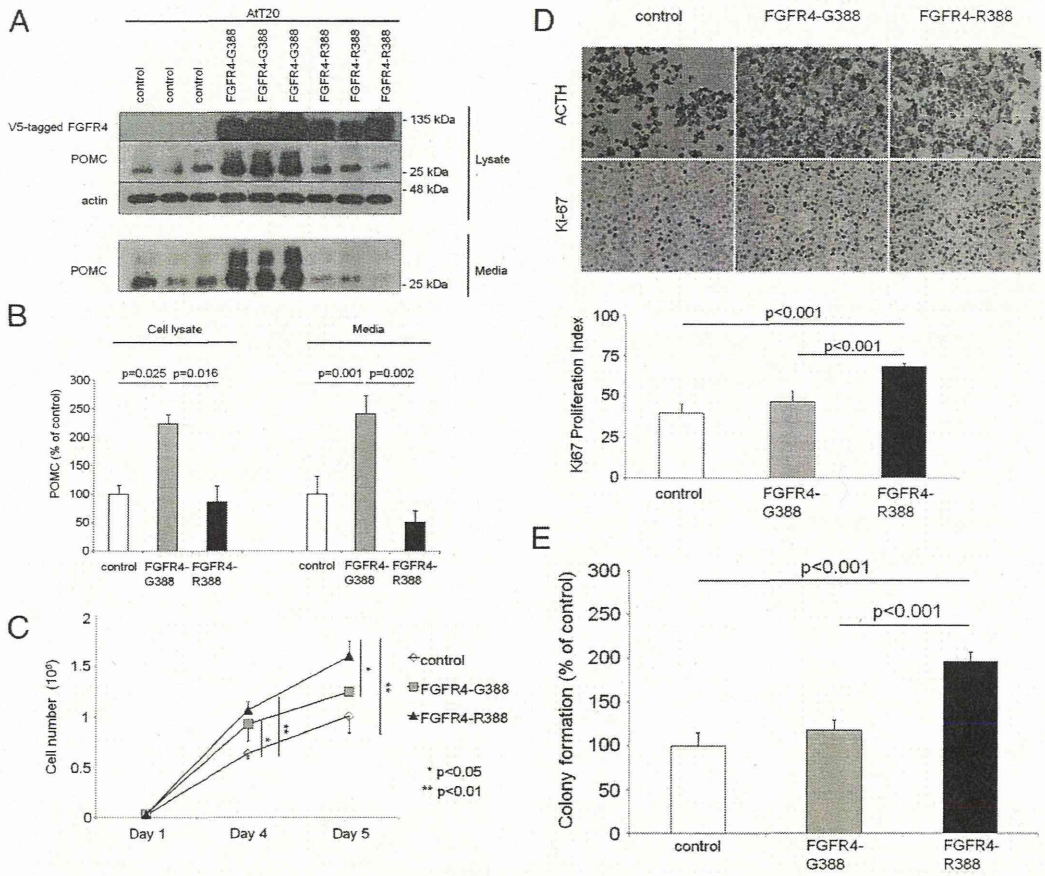


**Figure 1.** FGFR4 polymorphic variants modulate corticotroph hormone production and cellular growth. A, POMC protein expression was examined in mouse AtT20 corticotroph tumor cells stably expressing empty vector (control), the prototypic form of the FGFR4 receptor (G388), or the polymorphic FGFR4–R388 variant by Western blotting. B, Densitometric means derived from 3 independent experiments are shown in the corresponding bar graphs, and significant differences are shown. C, Growth of AtT20 cells expressing empty vector (control), FGFR4–G388, or FGFR4–R388 was monitored by counting the number of cells at 1, 4, and 5 days as detailed in *Materials and Methods*. Bar graphs indicate the average number of cells, based on 3 independent experiments each performed in triplicate. D, AtT20 cells expressing empty vector (control), FGFR4–G388, or FGFR4–R388 were stained for ACTH and Ki67. The proliferation index was calculated as the number of positive cells per 100 cells averaged in 3 areas of each slide, and significant differences are shown with corresponding statistical *P* values. Statistical comparisons were performed by ANOVA followed by post hoc analysis. E, AtT20 cells expressing empty vector (control), FGFR4–G388, or FGFR4–R388 were examined in soft agar as detailed in *Materials and Methods*. Shown is the change in the number of colonies (mean ± SD) derived from 4 independent experiments. Statistically significant ($P < .001$) increased colony numbers were noted as indicated. Statistical comparisons were performed by ANOVA followed by post hoc analysis.

pY-STAT3 levels, which were further enhanced by dexamethasone treatment (Figure 2, A and D). In contrast, dexamethasone did not further alter Src or STAT3 serine phosphorylation levels in either cell type. Moreover, introduction of a constitutively active serine STAT3 (STAT3-S727D) mutant enhanced colony formation, an effect not shared with a constitutively active tyrosine STAT3 (STAT3-CA) construct (Supplemental Figure 1B). STAT1 and STAT5 phosphorylation were not affected by either FGFR4 isoform (data not shown).

## FGFR4 isoform–mediated STAT3 signaling regulates POMC expression

Because glucocorticoids play a major role in negatively regulating their own expression through feedback inhibition of the pituitary-adrenal axis, we next tested responsiveness to dexamethasone. FGFR4-R388 cells showed enhanced dose-responsive inhibition of POMC to dexamethasone when compared with that of cells expressing the FGFR4-G388 variant (Figure 3, A and B) or control AtT20 cells (Supplemental Figure 2). To determine whether differential STAT3 modifications are responsible for pituitary POMC regulation, we tested AtT20 cells expressing constitutively active STAT3 mutants. Introduction of the tyrosine active STAT3-CA mimicked the effect of FGFR4-G388 with relative hormone insensitivity to dexamethasone (Figure 3, C and D). In contrast, introduction of a serine active form of STAT3 (STAT3-S727D) reproduced the enhanced suppression of POMC (Figure 3, C and D) noted in FGFR4-R388 cells.

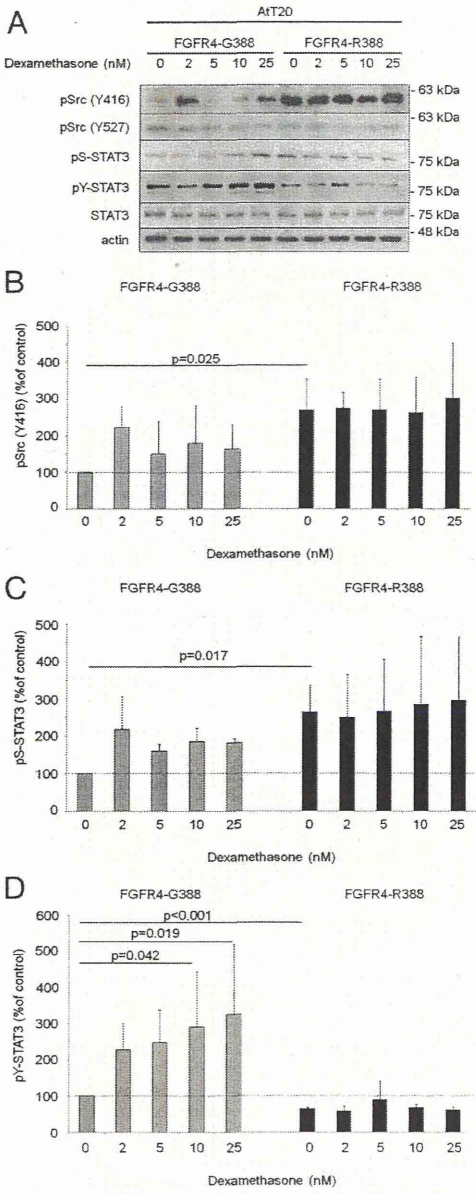


**Figure 2.** FGFR4 polymorphic variants display distinct signaling responses in pituitary corticotroph cells. A, AtT20 cells expressing FGFR4–G388 or FGFR4–R388 were treated with dexamethasone under serum-free defined conditions. Equal amounts of cell lysates were resolved by SDS-PAGE and analyzed by immunoblotting as indicated. Results are representative of 3 independent experiments. Values represent mean ± SD densitometric values derived from 3 independent experiments. Empty vector control cells are shown in Supplemental Figure 2. B–D, Bar graphs represent mean densitometric values derived from 3 independent experiments, and significant differences by *t* test (B and C) or ANOVA followed by post hoc analysis (D) are shown with corresponding *P* values.

## Distinct STAT3 modifications modulate phosphorylation and translocation of the GR

To understand the underlying mechanisms for altered FGFR4-STAT3–mediated POMC responsiveness, we examined GR phosphorylation and nuclear translocation (36). Of note, total GR levels were not altered in FGFR4-

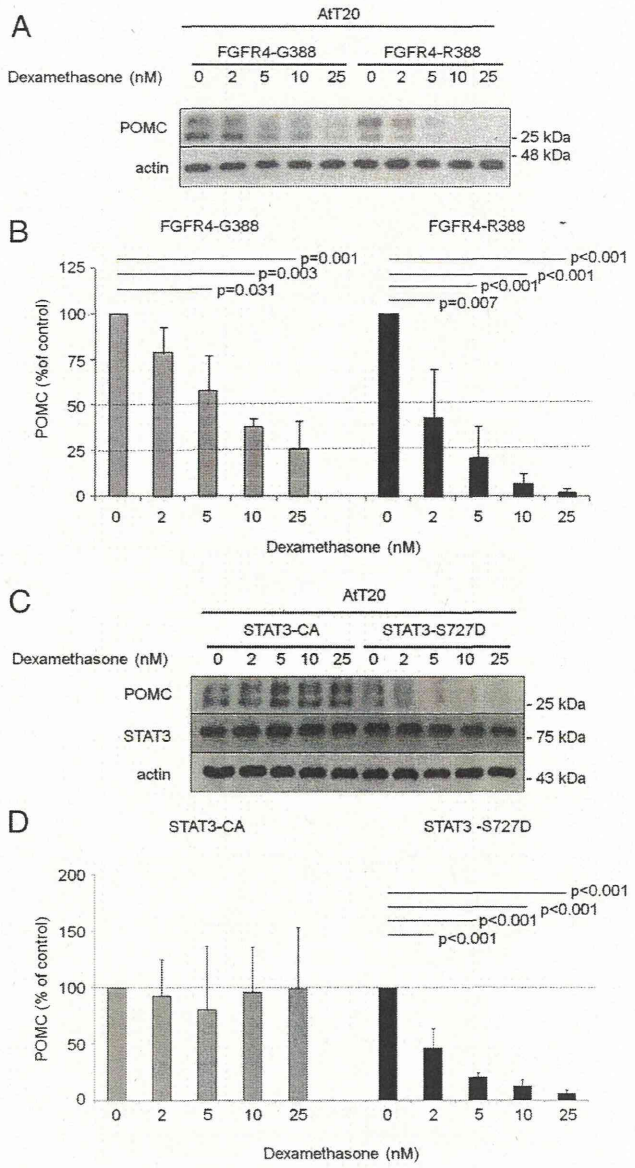


**Figure 3.** The FGFR4–R388 variant allele confers enhanced sensitivity to pituitary corticotroph hormone inhibition. A, AtT20 cells expressing empty vector (Supplemental Figure 1), FGFR4–G388, or FGFR4–R388 were treated with dexamethasone (0–25 nM) in serum-free defined media. Equal amounts of cell lysates were resolved by SDS-PAGE and analyzed by immunoblotting as indicated. Results are representative of 3 independent experiments. B, Bar graphs represent mean densitometric values derived from 3 independent experiments; significant differences are shown with corresponding *P* values determined by ANOVA followed by post hoc analysis. C, AtT20 cells expressing a tyrosine active form (STAT3-CA) and serine active form (STAT3–S727D) were treated with dexamethasone under serum-free defined conditions. Equal amounts of cell lysates were resolved by SDS-PAGE and immunoblotting detection for POMC, STAT3, and actin as indicated. D, Introduction of serine active STAT3–S727D shows dose-dependent enhanced sensitivity to dexamethasone inhibition. This effect is not shared with the tyrosine active STAT3-CA mutant. Bar graphs represent mean densitometric values derived from 3 independent experiments. Significant differences are shown with corresponding *P* values determined by ANOVA followed by post hoc analysis. Empty vector control cells are shown in Supplemental Figure 3.

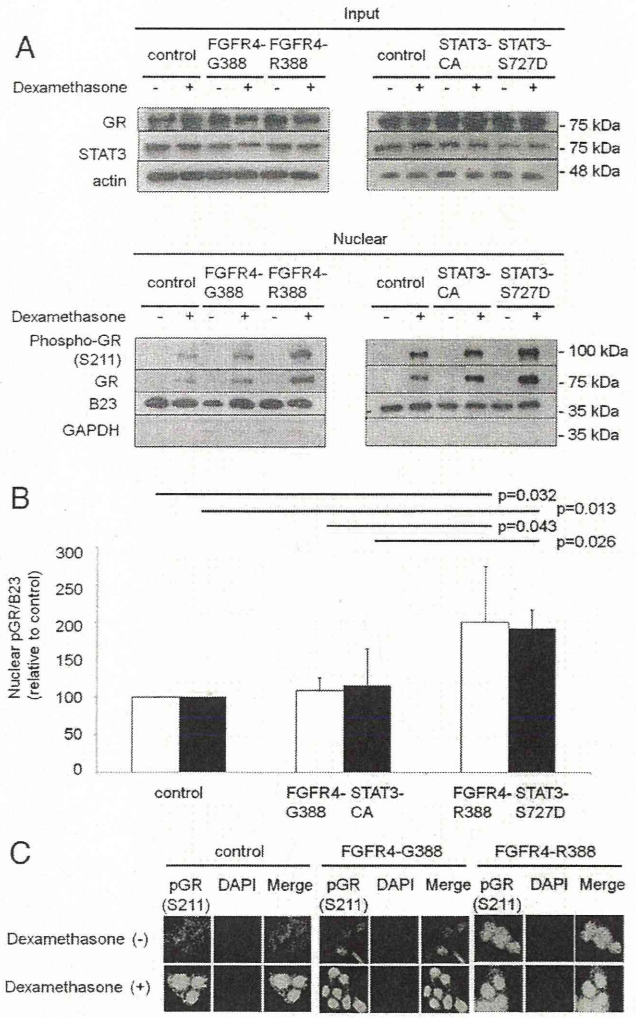


**Figure 4.** FGFR4–R388 enhances GR phosphorylation and nuclear translocation. A, AtT20 cells stably expressing vector control, FGFR4–G388, or FGFR4–R388 (left) and vector control, STAT3-CA, or STAT3–S727D (right) were treated with dexamethasone (10 nM) in serum-free defined media. Equal amounts of cell lysates were resolved by SDS-PAGE and immunoblotting detection for GR and actin as indicated (top panel). Nuclear protein fractions were resolved by SDS-PAGE and immunoblotted for GR and Ser211-phosphorylated nuclear GR (phospho-GR) (lower panel). B23 and GAPDH were used as markers for nuclear and cytoplasmic protein separations respectively. B, Quantification of nuclear pGR/B23 values from experiments shown in panel B were calculated relative to control cells. Values represent means ± SD obtained from 3 independent experiments. Significant differences are shown with corresponding *P* values determined by ANOVA followed by post hoc analysis. C, AtT20 cells expressing empty vector (control), FGFR4–G388, or FGFR4–R388 were fixed and stained with anti-pGR followed by Alexa 488-conjugated secondary antibody. Nuclei were stained with 4′,6-diamidino-2-phenylindole. Unlike FGFR4–R388 or control cells, FGFR4–G388 cells (middle) show diminished GR nuclear translocation after dexamethasone treatment. DAPI, 4′,6-diamidino-2-phenylindole.

G388 and FGFR4-R388 cells as determined by whole-cell lysate Western blotting (Figure 4A, top). Examination of fractionated proteins identified enhanced pGR responsiveness to dexamethasone in FGFR4-R388 cells (Figure 4A, bottom). Moreover, introduction of the serine active STAT3-S727D recapitulated the enhancing effect on pGR (Figure 4, A and B). In contrast, introduction of the tyrosine constituently active STAT3 (STAT3-CA) failed to reproduce this impact on GR responses (Figure 4, A and B). Tracking immunofluorescence studies corroborated the diminished pGR nuclear translocation after dexamethasone treatment in FGFR4-G388 cells compared with that in FGFR-R388 cells (Figure 4C).

## Knock-in of the mouse FGFR4 R385 variant alleles modulates POMC negative feedback inhibition in vivo

To determine whether the observed cellular responses displayed by the FGFR4 polymorphic variants translate into biologically relevant actions on pituitary cell growth and function, we examined mice with knock-in of the mouse homolog of the polymorphism, FGFR4-R385. Of note, knock-in of this variant allele does not alter FGFR4 expression levels (26, 35).

To determine whether the FGFR4 variant allele influences POMC negative feedback inhibition, we performed dexamethasone suppression testing on FGFR4-G385 (G/G) controls, mice carrying one copy of the variant allele (G/R), and homozygote (R/R) knock-in mice. Dexamethasone treatment significantly decreased plasma corticosterone levels in heterozygous mice and homozygote mice (Figure 5). Consistent with the in vitro findings, mice carrying an FGFR4-R385 allele demonstrated significantly greater glu-

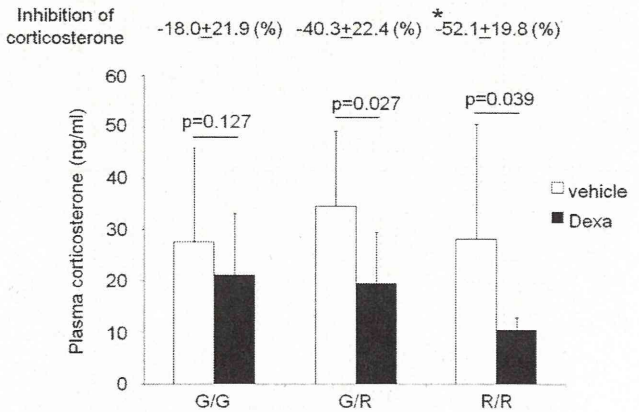


**Figure 5.** Knock-in of the mouse FGFR4–R385 variant allele enhances POMC negative feedback inhibition in vivo. The dexamethasone (Dexa) suppression test was performed on FGFR4–G385 (G/G), heterozygote (G/R), and homozygote (R/R) knock-in mice. Plasma corticosterone levels before and after the dexamethasone test were measured by ELISA. Significant differences are depicted with corresponding *P* values by *t* test comparisons within each group. Mice carrying an FGFR4–R385 allele demonstrated greater glucocorticoid inhibition than mice homozygous for the FGFR4–G385 allele with the degrees of inhibition shown immediately above. *, $P = .035$, significant differences compared with wild-type mice, determined by ANOVA followed by post hoc analysis.

**Table 1.** Association Between FGFR4 Alleles, Clinical Diagnosis, and Corticotroph Tumor Size

| FGFR4 Allele | G/G, n (%) | G/R, n (%) | R/R, n (%) | *P* |
|---|---|---|---|---|
| Patients | 21 (30.0) | 41 (58.6) | 8 (11.4) | |
| Clinical diagnosis | | | | |
| CD | 20 (95.2) | 40 (97.6) | 5 (62.5) | .0018 |
| SCA | 1 (4.8) | 1 (2.4) | 3 (37.5) | |
| Tumor size | | | | |
| Microadenomas | 17 (81.0) | 31 (75.6) | 3 (37.5) | .0521 |
| Macroadenomas | 4 (19.0) | 10 (24.4) | 5 (62.5) | |
| Invasiveness | | | | |
| Invasive | 7 (33.3) | 15 (36.6) | 4 (50) | .7038 |
| Noninvasive | 14 (66.7) | 26 (63.4) | 4 (50) | |
| Corticotroph adenoma subtype | | | | |
| DG | 19 (90.5) | 32 (78.0) | 3 (37.5) | .0317 |
| SG | 2 (9.5) | 8 (19.5) | 5 (62.5) | |
| Mixed | 0 | 1 (2.5) | 0 | |

Abbreviations: CD, Cushing disease; DG, densely granulated adenoma; SG, sparsely granulated adenoma.

cocorticoid inhibition of adrenal corticosterone levels ($-52.1 \pm 19.8\%$ vs $-18.0 \pm 21.9\%$; $n = 7$, $P = .035$) than control mice homozygous for the FGFR4-G385 allele (Figure 5).

### FGFR4-G388R alters clinical pituitary corticotroph tumor phenotype

Given the ability of FGFR4 isoforms to display different effects on the POMC-ACTH axis, we sought to identify evidence linking these 2 processes in human disease. Of 70 patients with pituitary corticotroph tumors, 21 (30.0%) were FGFR4-G388, 41 patients (58.6%) harbored 1 FGFR4-R388 allele, and 8 patients (11.4%) were FGFR4-R388 homozygous (Table 1). Interestingly, the diagnosis of Cushing disease was made in >95% of patients harboring an FGFR4-G388 allele compared with only 62.5% of patients homozygous for FGFR4-R388 ($P = .0018$). As shown in Table 1, there was also a significant correlation between the FGFR4-R388 allele and pituitary tumor size ($P = .0521$). Of 21 patients homozygous for FGFR4-G388, 17 (81%) had microadenomas and 4 (19%) had macroadenomas. Among 41 heterozygotes, 31 (75.6%) had microadenomas. In contrast, of the 8 patients homozygous for the R/R allele, only 3 (37.5%) had microadenomas and 5 (62.5%) had macroadenomas. There was also a statistically significant difference in morphology among the genotypes. Patients with an FGFR4-G388 allele more often had basophilic densely granulated tumors, whereas FGFR4-R388 homozygotes were more likely to have chromophobic sparsely granulated tumor cells ($P = .0317$). Interestingly, all 5 tumors that exhibited Crooke's hyaline change (the morphologic hallmark of glucocorticoid-mediated inhibition) were associated with an FGFR4-R388 genotype.

These data support a link between the FGFR4-G388 allele and increased ACTH production by characteristically small microadenomas of Cushing disease. In contrast, the FGFR4-R388 variant allele restrains POMC-ACTH hormone production but supports the more aggressive growth characteristic of sparsely granulated corticotroph macroadenomas and silent corticotroph adenomas.

## Discussion

The FGFR4-R388 polymorphic allele can alter susceptibility to some cancers, modulate patient outcome in different types of cancers (37), and result in differences in disease outcomes or responses to therapy (25). However, the mechanisms underlying these actions continue to emerge. The 2 FGFR4 isotypes have divergent signaling properties in different tissues as demonstrated in breast (38), pancreas (25, 39), and mammosomatotroph cells (26). We show here that compared with the polymorphic FGFR4-R388 variant, the prototypic form of the receptor (FGFR4-G388) enhances corticotroph hormone production and confers relative resistance to dexamethasone-mediated POMC inhibition without increasing cell growth.

Consistent with our previous findings in GH-producing cells (26), FGFR4-R388 signaling is accompanied by enhanced Src and STAT3 activation in AtT20 cells. In particular, the pituitary FGFR4-R388 variant relies on serine (S727) but not tyrosyl (Y705) phosphorylation of STAT3. The current study implies multiple consequences of these altered STAT3 modifications in the control of pituitary hormonal balance. STAT3, a member of the Janus kinase/STAT family, is a transcription factor that, after activation, binds to specific sequences in DNA to regulate expression of genes related to proliferation, differentiation, and cell survival. Interestingly, STAT3 can physically interact with the GR as noted in hepatocytes, B cells, and kidney cells (40–42). Here we show that FGFR4-G388 cells support pY-STAT3 signaling, resulting in increased POMC expression with relative resistance to dexamethasone inhibition. This effect was ascribed to diminished GR phosphorylation and consequently nuclear translocation. Further, these properties were recapitulated by introducing a constitutively active pY-STAT3 mutant.

Direct protein-protein interaction between STAT3 and GR using coimmunoprecipitation experiments has been described (40), suggesting that STAT3 might be involved directly in the transcriptional activity elicited by GR. Using fractionation studies, we found diminished nuclear translocation of the phosphorylated Ser211 GR in AtT20

cells expressing the FGFR4-G388 compared with those expressing the FGFR4-R388, an effect that was recapitulated by expressing a tyrosine active STAT3 mutant. Most GR-mediated signaling indirectly regulate target genes by influencing intermediary transcription factors such as STAT3 and STAT5 (40). For example, leukemia inhibitory factor administration reduces GR expression in AtT20 cells through STAT3-dependent signaling (43). However, there are probably several mechanisms involved in STAT3-mediated GR resistance (44–46). Our current data link FGFR4 polymorphic variants with distinct STAT3 modifications that modulate GR activation.

In contrast to the impact of FGFR4-G388 on pY-STAT3, FGFR4-R388 was coupled to serine STAT3 phosphorylation (pS727-STAT3). STAT3 is generally regarded as a requirement for Src-mediated cell transformation as shown in many carcinomas (47). Traditionally, STAT3 oncogenic functions have been regarded to rely on pY-STAT3 and its nuclear translocation. However, recent studies have also identified a positive impact of pS727-STAT3 on cell transformation. Unlike the tyrosine modification, serine-phosphorylated STAT3 has been described in the mitochondria (48). It may also be involved in the negative modulation of STAT3 tyrosine phosphorylation (49). Our previous data showed that the FGFR4-R388 promotes mitochondrial STAT3 serine phosphorylation through Src, resulting in increased cell proliferation and GH production (26). Here we show that in corticotroph AtT20 cells, the FGFR4 polymorphic R388 variant activates Src and STAT3 serine phosphorylation, leading to increased cellular growth. This effect was recapitulated with introduction of a constitutively active serine STAT3 but not by a tyrosine active mutant.

Our studies of mice with knock-in of the murine homolog of the human FGFR4-R388 allele (FGFR4-R385) support the hypothesis of altered sensitivity to dexamethasone-mediated POMC negative feedback. Indeed, mice with knock-in of the FGFR4-R385 allele displayed nearly twice the degree of glucocorticoid inhibition by dexamethasone. Mice carrying the FGFR4-R385 allele do not develop pituitary corticotroph tumors spontaneously, implicating other factors in the neoplastic transformation of this pituitary cell lineage; thus, the FGFR4 single nucleotide polymorphism acts as a modifier of tumor cell behavior.

We show that the FGFR4-G388R polymorphism affects human corticotroph adenoma behavior. Clinical data from patients with ACTH-producing pituitary tumors revealed that those homozygous for the R388 allele have a higher frequency of SCAs and macroadenomas with subtle features of hypercortisolemia compared with carriers of the G388 allele who were more likely to have microadenomas causing florid Cushing disease. These data are consistent with earlier observations that homozygosity for FGFR4-G388 is associated with a higher frequency of persistence of cortisol hypersecretion in surgically treated patients with Cushing disease (27).

In summary, we show that the heritable FGFR4-R388 allele yields a receptor variant that signals in a manner distinct from that of its prototypic FGFR4-G388 isoform in pituitary corticotroph cells. With the ability to respond through distinct STAT3 modifications, the variant isoform FGFR4-R388 allele promotes cellular growth while enhancing GR activity and thereby sensitivity to hormone negative feedback inhibition. These findings identify the common FGFR4 polymorphism as a factor contributing to characteristic clinicopathological features associated with diseases of the pituitary corticotroph.

## Acknowledgments

We thank Dr Axel Ullrich for providing FGFR4 reagents and mice and for helpful discussions. We also thank Anastasia Diamandis for technical assistance with immunoassays.

Address all correspondence and requests for reprints to: Dr. S. Ezzat, Ontario Cancer Institute, 610 University Avenue 8-327, Toronto, ON, Canada M5G-2M9. E-mail: shereen.ezzat@utoronto.ca.

This work was supported by the Canadian Institutes of Health Research (CIHR-MOP-125981), the John and Myrna Daniels Endocrine Cancer Research Fund, and the Ontario Ministry of Health and Long-Term Care (OMHLTC). The views expressed do not necessarily reflect those of the OMHLTC.

Disclosure Summary: The authors have nothing to disclose.

## References

1. **Ezzat S, Asa SL, Couldwell WT, et al.** The prevalence of pituitary adenomas: a systematic review. *Cancer*. 2004;101:613–619.
2. **Asa SL, Ezzat S.** The pathogenesis of pituitary tumors. *Annu Rev Pathol*. 2009;4:97–126.
3. **Asa SL, Ezzat S.** The pathogenesis of pituitary tumours. *Nat Rev Cancer*. 2002;2:836–849.
4. **Chandrasekharappa SC, Guru SC, Manickam P, et al.** Positional cloning of the gene for multiple endocrine neoplasia-type 1. *Science*. 1997;276:404–407.
5. **Zhuang Z, Ezzat SZ, Vortmeyer AO, et al.** Mutations of the MEN1 tumor suppressor gene in pituitary tumors. *Cancer Res*. 1997;57:5446–5451.
6. **Daly AF, Vanbellinghen JF, Khoo SK, et al.** Aryl hydrocarbon receptor-interacting protein gene mutations in familial isolated pituitary adenomas: analysis in 73 families. *J Clin Endocrinol Metab*. 2007;92:1891–1896.
7. **Kirschner LS, Carney JA, Pack SD, et al.** Mutations of the gene encoding the protein kinase A type I-α regulatory subunit in patients with the Carney complex. *Nat Genet*. 2000;26:89–92.
8. **Scully KM, Rosenfeld MG.** Pituitary development: regulatory codes in mammalian organogenesis. *Science*. 2002;295:2231–2235.
9. **De Moerlooze L, Spencer-Dene B, Revest JM, Hajihosseini M, Rosewell I, Dickson C.** An important role for the IIIb isoform of

fibroblast growth factor receptor 2 (FGFR2) in mesenchymal-epithelial signalling during mouse organogenesis. *Development*. 2000; 127:483–492.
10. **Ezzat S, Kontogeorgos G, Redelmeier DA, Horvath E, Harris AG, Kovacs K.** In vivo responsiveness of morphological variants of growth hormone-producing pituitary adenomas to octreotide. *Eur J Endocrinol*. 1995;133:686–690.
11. **Ezzat S, Smyth HS, Ramyar L, Asa SL.** Heterogenous in vivo and in vitro expression of basic fibroblast growth factor by human pituitary adenomas. *J Clin Endocrinol Metab*. 1995;80:878–884.
12. **Abbass SA, Asa SL, Ezzat S.** Altered expression of fibroblast growth factor receptors in human pituitary adenomas. *J Clin Endocrinol Metab*. 1997;82:1160–1166.
13. **Ezzat S, Zheng L, Zhu XF, Wu GE, Asa SL.** Targeted expression of a human pituitary tumor-derived isoform of FGF receptor-4 recapitulates pituitary tumorigenesis. *J Clin Invest*. 2002;109:69–78.
14. **Yu S, Asa SL, Weigel RJ, Ezzat S.** Pituitary tumor AP-2$\alpha$ recognizes a cryptic promoter in intron 4 of fibroblast growth factor receptor 4. *J Biol Chem*. 2003;278:19597–19602.
15. **Ezzat S, Yu S, Asa SL.** Ikaros isoforms in human pituitary tumors: distinct localization, histone acetylation, and activation of the 5′ fibroblast growth factor receptor-4 promoter. *Am J Pathol*. 2003; 163:1177–1184.
16. **Qian ZR, Sano T, Asa SL, et al.** Cytoplasmic expression of fibroblast growth factor receptor-4 in human pituitary adenomas: relation to tumor type, size, proliferation, and invasiveness. *J Clin Endocrinol Metab*. 2004;89:1904–1911.
17. **Bange J, Prechtl D, Cheburkin Y, et al.** Cancer progression and tumor cell motility are associated with the FGFR4 Arg(388) allele. *Cancer Res*. 2002;62:840–847.
18. **Morimoto Y, Ozaki T, Ouchida M, et al.** Single nucleotide polymorphism in fibroblast growth factor receptor 4 at codon 388 is associated with prognosis in high-grade soft tissue sarcoma. *Cancer*. 2003;98:2245–2250.
19. **Wang J, Stockton DW, Ittmann M.** The fibroblast growth factor receptor-4 Arg388 allele is associated with prostate cancer initiation and progression. *Clin Cancer Res*. 2004;10:6169–6178.
20. **Falvella FS, Frullanti E, Galvan A, et al.** FGFR4 Gly388Arg polymorphism may affect the clinical stage of patients with lung cancer by modulating the transcriptional profile of normal lung. *Int J Cancer*. 2009;124:2880–2885.
21. **Sasaki H, Okuda K, Kawano O, Yukiue H, Yano M, Fujii Y.** Fibroblast growth factor receptor 4 mutation and polymorphism in Japanese lung cancer. *Oncol Rep*. 2008;20:1125–1130.
22. **da Costa Andrade VC, Parise O Jr, Hors CP, de Melo Martins PC, Silva AP, Garicochea B.** The fibroblast growth factor receptor 4 (FGFR4) Arg388 allele correlates with survival in head and neck squamous cell carcinoma. *Exp Mol Pathol*. 2007;82:53–57.
23. **Streit S, Mestel DS, Schmidt M, Ullrich A, Berking C.** FGFR4 Arg388 allele correlates with tumour thickness and FGFR4 protein expression with survival of melanoma patients. *Br J Cancer*. 2006; 94:1879–1886.
24. **Thussbas C, Nahrig J, Streit S, et al.** FGFR4 Arg388 allele is associated with resistance to adjuvant therapy in primary breast cancer. *J Clin Oncol*. 2006;24:3747–3755.
25. **Serra S, Zheng L, Hassan M, et al.** The FGFR4–G388R single-nucleotide polymorphism alters pancreatic neuroendocrine tumor progression and response to mTOR inhibition therapy. *Cancer Res*. 2012;72:5683–5691.
26. **Tateno T, Asa SL, Zheng L, et al.** The FGFR4–G388R polymorphism promotes mitochondrial STAT3 serine phosphorylation to facilitate pituitary growth hormone cell tumorigenesis. *PLoS Genet*. 2011;7:e1002400.
27. **Brito LP, Lerário AM, Bronstein MD, Soares IC, Mendonca BB, Fragoso MC.** Influence of the fibroblast growth factor receptor 4 expression and the G388R functional polymorphism on Cushing's disease outcome. *J Clin Endocrinol Metab*. 2010;95:E271–E279.
28. **Nieman LK, Biller BM, Findling JW, et al.** The diagnosis of Cushing's syndrome: an Endocrine Society Clinical Practice Guideline. *J Clin Endocrinol Metab*. 2008;93:1526–1540.
29. **Asa SL** *Tumors of the Pituitary Gland*. Washington, DC: Armed Forces Institute of Pathology; 2011. The Atlas of Tumor Pathology. Fascicle 15, 4th Series.
30. **Cooper O, Ben-Shlomo A, Bonert V, Bannykh S, Mirocha J, Melmed S.** Silent corticogonadotroph adenomas: clinical and cellular characteristics and long-term outcomes. *Horm Cancer*. 2010;1:80–92.
31. **Baldeweg SE, Pollock JR, Powell M, Ahlquist J.** A spectrum of behaviour in silent corticotroph pituitary adenomas. *Br J Neurosurg*. 2005;19:38–42.
32. **Yamada S, Ohyama K, Taguchi M, et al.** A study of the correlation between morphological findings and biological activities in clinically nonfunctioning pituitary adenomas. *Neurosurgery*. 2007;61:580–585.
33. **Mete O, Ezzat S, Asa SL.** Biomarkers of aggressive pituitary adenomas. *J Mol Endocrinol*. 2012;49:R69–R78.
34. **Kim JH, Yoon MS, Chen J.** Signal transducer and activator of transcription 3 (STAT3) mediates amino acid inhibition of insulin signaling through serine 727 phosphorylation. *J Biol Chem*. 2009; 284:35425–35432.
35. **Seitzer N, Mayr T, Streit S, Ullrich A.** A single nucleotide change in the mouse genome accelerates breast cancer progression. *Cancer Res*. 2010;70:802–812.
36. **Ismaili N, Garabedian MJ.** Modulation of glucocorticoid receptor function via phosphorylation. *Ann NY Acad Sci*. 2004;1024:86–101.
37. **Frullanti E, Berking C, Harbeck N, et al.** Meta and pooled analyses of FGFR4 Gly388Arg polymorphism as a cancer prognostic factor. *Eur J Cancer Prev*. 2011;20:340–347.
38. **Stadler CR, Knyazev P, Bange J, Ullrich A.** FGFR4 GLY388 isotype suppresses motility of MDA-MB-231 breast cancer cells by EDG-2 gene repression. *Cell Signal*. 2006;18:783–794.
39. **Ezzat S, Zheng L, Florez JC, et al.** The cancer-associated FGFR4–G388R polymorphism enhances pancreatic insulin secretion and modifies the risk of diabetes. *Cell Metab*. 2013;17:929–940.
40. **Zhang Z, Jones S, Hagood JS, Fuentes NL, Fuller GM.** STAT3 acts as a co-activator of glucocorticoid receptor signaling. *J Biol Chem*. 1997;272:30607–30610.
41. **Unterberger C, Staples KJ, Smallie T, et al.** Role of STAT3 in glucocorticoid-induced expression of the human IL-10 gene. *Mol Immunol*. 2008;45:3230–3237.
42. **De Miguel F, Lee SO, Onate SA, Gao AC.** Stat3 enhances transactivation of steroid hormone receptors. *Nucl Recept*. 2003;1:3.
43. **Kariagina A, Zonis S, Afkhami M, Romanenko D, Chesnokova V.** Leukemia inhibitory factor regulates glucocorticoid receptor expression in the hypothalamic-pituitary-adrenal axis. *Am J Physiol Endocrinol Metab*. 2005;289:E857–E863.
44. **Korbonits M, Bujalska I, Shimojo M, et al.** Expression of 11 $\beta$-hydroxysteroid dehydrogenase isoenzymes in the human pituitary: induction of the type 2 enzyme in corticotropinomas and other pituitary tumors. *J Clin Endocrinol Metab*. 2001;86:2728–2733.
45. **Antonini SR, Latronico AC, Elias LL, et al.** Glucocorticoid receptor gene polymorphisms in ACTH-secreting pituitary tumours. *Clin Endocrinol (Oxf)*. 2002;57:657–662.
46. **Bilodeau S, Vallette-Kasic S, Gauthier Y, et al.** Role of Brg1 and HDAC2 in GR trans-repression of the pituitary POMC gene and misexpression in Cushing disease. *Genes Dev*. 2006;20:2871–2886.
47. **Yu H, Jove R.** The STATs of cancer—new molecular targets come of age. *Nat Rev Cancer*. 2004;4:97–105.
48. **Gough DJ, Corlett A, Schlessinger K, Wegrzyn J, Larner AC, Levy DE.** Mitochondrial STAT3 supports Ras-dependent oncogenic transformation. *Science*. 2009;324:1713–1716.
49. **Chung J, Uchida E, Grammer TC, Blenis J.** STAT3 serine phosphorylation by ERK-dependent and -independent pathways negatively modulates its tyrosine phosphorylation. *Mol Cell Biol*. 1997; 17:6508–6516.

CASE REPORT doi: 10.2176/nmc.cr.2013-0008
Neurol Med Chir (Tokyo) 54, 629–633, 2014 Online January 10, 2014

# Clinical Characteristics of Streptococcus Pneumoniae Meningoencephalitis after Transsphenoidal Surgery: Three Case Reports

Nobuyuki KOBAYASHI,[1,2] Noriaki FUKUHARA,[1] Takahito FUKUI,[1] Mitsuo YAMAGUCHI-OKADA,[1,3] Hiroshi NISHIOKA,[1,4] and Shozo YAMADA[1,4]

[1]*Department of Hypothalamic and Pituitary Surgery, Toranomon Hospital, Tokyo;*
[2]*Department of Neurosurgery, Yuuai Memorial Hospital, Koga, Ibaraki;*
[3]*Department of Neurosurgery, Seirei Yokohama Hospital, Yokohama, Kanagawa;*
[4]*Okinaka Memorial Institute for Medical Research, Toranomon Hospital, Tokyo*

## Abstract

**We report three extremely rare cases of *Streptococcus pneumoniae* meningoencephalitis (SPM) after transsphenoidal surgery (TSS). Between 2004 and 2010, we experienced three cases of severe SPM after surgery out of 1,965 patients undergoing TSS (0.15%). The three cases included a 4-year-old boy with a large cystic craniopharyngioma, a 40-year-old man with a non-functioning pituitary adenoma, and a 55-year-old man with acromegaly. The similarity among these SPM patients was that severe clinical events occurred suddenly 1–2 months postoperatively without any history of sinusitis or pneumonia. Despite intensive care these patients notably had residual neurological sequelae. In no case was rhinorrhea associated with SPM. It should be noted that SPM was not detected from bacterial cultures of the sphenoidal sinus mucous membranes (BCSM) obtained during TSS in two of the patients examined. Severe postoperative SPM can occur suddenly without cerebrospinal fluid (CSF) leakage within 2 months after surgery and requires emergency treatment. Reduced resistance to infection may play a role in the occurrence of SPM in our three patients. Our study indicates that BCSM is not useful for predicting postoperative meningitis.**

Key words: complications, meningoencephalitis, pituitary tumors, *Streptococcus pneumoniae*, transsphenoidal surgery

## Introduction

Bacterial meningitis is a severe complication of transsphenoidal surgery (TSS) for pituitary tumors[1–3] with an incidence ranging from 0.4% to 9%.[3] For instance, Van Aken et al. mentioned an incidence of 3.1% after TSS (7 of 228 cases)[3] and described five gram-positive bacteria including two species of *Staphylococcus aureus*, and one species each of *Streptococcus (Str.) sanguis*, *Str. intermedius*, and *Enterococcus* species[3]. In contrast, only two of 316 consecutive patients who underwent TSS or extended TSS between January 2006 and July 2007 (0.63%) at our institution were diagnosed with postoperative meningitis, demonstrating a lower incidence of postoperative meningitis in our department compared with others.[2,3] However, meningoencephalitis due to *Str. pneumoniae* is considered extremely rare, and to our knowledge only one patient has been reported in the English literature with this disease.[1] Therefore, the clinical characteristics of *Streptococcus pneumoniae* meningoencephalitis (SPM) associated with TSS remain to be elucidated. We have experienced three cases of SPM after TSS between 2004 and 2010, which accounts for 0.15% of the 1,965 cases of TSS performed for the treatment of various types of pituitary diseases at Toranomon Hospital, including pituitary adenomas, craniopharyngiomas, and Rathke's cleft cysts. Here, we report these three cases of SPM to clarify the clinical characteristics of postoperative SPM after TSS.

Received January 10, 2013; Accepted July 29, 2013

## Case Report

### I. Case 1: Large cystic craniopharyngioma, 4-year-old male (Fig. 1A, B)

The patient complained of visual disturbance with impaired eye movements. Magnetic resonance (MR) imaging

showed a large, cystic, dumbbell-shaped craniopharyngioma. He underwent complete tumor excision via extended TSS in October 2009. Cerebrospinal fluid (CSF) leakage was unavoidable during surgery due to the extended approach, and a large dural defect was reconstructed with a dural fascia graft followed by subcutaneous adipose tissue and fibrin glue to prevent postoperative CSF leakage.[4] The patient received prophylactic antibiotics [cefazoline sodium (CEZ)] for 7 days. The patient was necessary refilled hydrocortisone, levothyroxine, and desmopressin after surgery. The postoperative course was unremarkable, there was no CSF leakage, and the patient was discharged 1 month after surgery with hormonal replacement for panhypopituitarism with diabetes insipidus. No laboratory data suggested inflammation at the time of discharge. However, 1 month after discharge (i.e., 2 months after surgery) the patient demonstrated high fever (up to 39°C) and generalized convulsions. He was diagnosed with SPM due to his clinical symptoms (e.g., high fever, neck stiffness) and CSF examination (cell counts: 2,530 μL, protein: 134 mg/dl, glucose: 12 mg/dl), which included a bacterial culture.

On the following day the patient was in critical condition with a severe disturbance of consciousness and convulsions. The patient recovered after intensive treatment with appropriate antibiotics, but he suffered cortical blindness secondary to an occipital infarction due to arterial vasculitis after SPM.

**II. Case 2: Non-functioning adenoma, 40-year-old man (Fig. 1C)**

The patient had a past history of repeat TSS at another hospital for the treatment of a non-functioning pituitary adenoma. During the second surgery severe intraoperative bleeding from the cavernous sinus occurred which resulted in severe postoperative anemia [hemoglobin (Hb) was reduced to 6.8 g/dl]. A repeat TSS was performed in July 2004 at Toranomon Hospital, and the tumor was completed removed without any intraoperative CSF leakage. He received prophylactic antibiotics (CEZ) for 3 days, and his postoperative course was uneventful. For this patient, postoperative hormonal replacement was not required. He was then discharged 10 days after surgery with slight anemia (Hb: 11 g/dl). The patient suddenly complained of severe headache 2 weeks after discharge (1 month after TSS) with a high fever followed by generalized convulsions. He was taken to the hospital by ambulance 2 days after the onset of high fever. He was comatose, and although a computed tomography (CT) scan did not show pneumocephalus, it did demonstrate diffuse brain swelling with multiple infarctions. Subsequent bacterial culture of the CSF revealed SPM (additional data from the CSF are not available). The patient died 2 weeks later despite intensive treatment for SPM. Neither CSF leakage nor pneumocephalus were found during the course of his meningoencephalitis. Bacterial cultures of the sphenoidal sinus mucous membrane (BCSM) performed at Toranomon Hospital confirmed no *Str. pneumoniae*, although both *Staphylococcus* species and *Klebsiella pneumonia* were detected in the membranes.

**III. Case 3: Acromegaly, 55-year-old man (Fig. 1D, E)**

This patient, a blue-collar worker, was diagnosed with acromegaly based on clinical and endocrinological findings. TSS was performed to remove the entire pituitary adenoma and to achieve an endocrinological cure at Toranomon Hospital in May 2004. (For this patient, postoperative hormonal replacement was not required.)

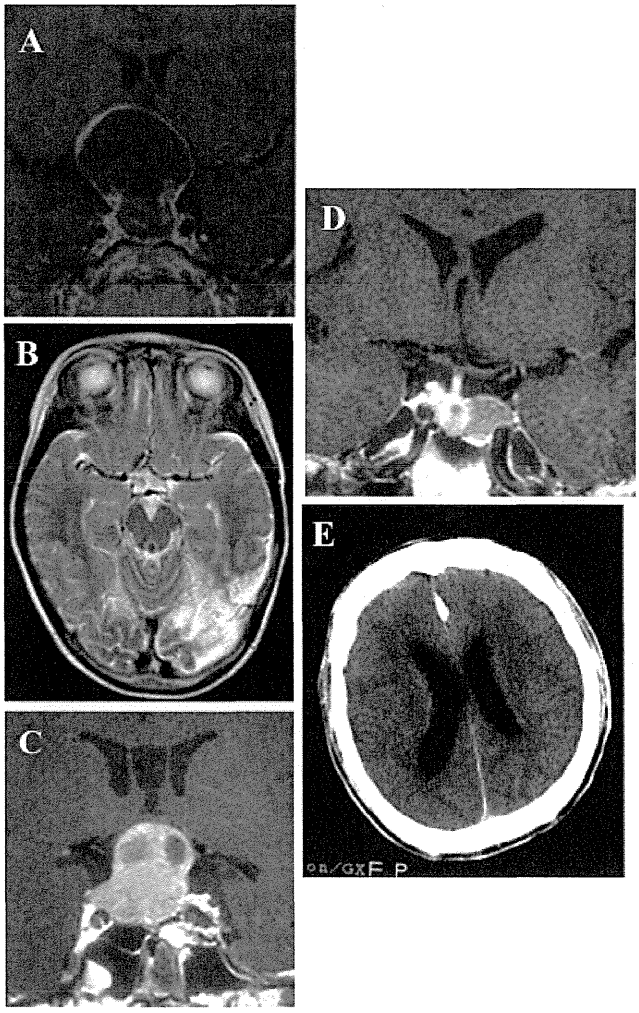


**Fig. 1 A, B: A 4-year-old boy with craniopharyngioma. A: Preoperative MR imaging (Gd-enhanced $T_1$WI) reveal a large, cystic, dumbbell-shaped tumor. B: $T_2$WI revealed left occipital infarction due to postoperative SPM. C: A 40-year-old man with non-functioning adenoma. D, E: A 55-year-old man with acromegaly. D: Preoperative MR imaging E: CT revealed brain edema due to SPM. CT: computed tomography, MR: magnetic imaging, SPM: *Streptococcus pneumoniae* meningoencephalitis.**